UNITED STATES DEPARTMENT OF THE INTERIOR

GEOLOGICAL SURVEY

# HYPOGENE MINERALOGY AND PARAGENESIS OF THE BALD MOUNTAIN MASSIVE SULFIDE DEPOSIT, AROOSTOOK COUNTY, MAINE

By

John F. Slack, Marta J.K. Flohr*

U.S. Geological Survey, National Center, MS 954, Reston, VA 20192

and

Michael V. Scully

Northeast Geophysical Services, 4 Union Street, Suite 3, Bangor, ME 04401

*Present address: 6588 Ox Road, Fairfax Station, VA 22039

Open-File Report 97-746



December, 1997

# INTRODUCTION

The Bald Mountain Cu-Zn-Au-Ag deposit is a large volcanogenic massive sulfide (VMS) body located in Aroostook County, northern Maine (Fig. 1). Bald Mountain is one of several VMS deposits known in northern New England that are hosted by early Paleozoic marine volcanic sequences (Gair and Slack, 1979, 1980; Stephens et al., 1984; Feiss and Slack, 1989; Fyffe et al., 1990; McCutcheon, 1993). Such deposits form by the precipitation of base metal sulfides (Cu ± Zn ± Pb) and locally precious metals (Ag ± Au) from metalliferous hydrothermal fluids on or beneath the seafloor, generally in the vicinity of submarine volcanic centers (e.g., Lydon, 1988; Franklin, 1993, 1995). Most ancient VMS deposits are deformed and metamorphosed to some extent, so that original textures, mineral assemblages, and mineral compositions are obscured or destroyed, with the result that generally only limited evidence can be obtained on primary mineralizing processes. The Bald Mountain deposit is very unusual among ancient VMS deposits in lacking a penetrative deformational fabric and being only weakly metamorphosed. Bald Mountain probably is the most pristine large VMS deposit in North America, and as such is ideally suited to detailed mineralogic and paragenetic investigations. In particular, the excellent preservation of original seafloor-hydrothermal textures there makes this a very important deposit to study.

The Bald Mountain deposit was discovered in 1977 by J.S. Cummings during a regional geochemical survey (Cummings, 1988). Exploration work at and surrounding the property since then has been carried out by several companies, including (from earliest to most recent): Superior Mining Company, Freeport Exploration Company, Chevron Resources Company, Boliden Resources Inc., and Black Hawk Mining Inc. The deposit consists of a large hypogene sulfide body overlain successively by a small supergene zone and a shallow gossan. The hypogene sulfide body comprises two major zones, a lower copper-rich zone that contains 20.4 million metric tonnes (Mt) of mineralized rock at an average grade of 1.64 % Cu and 0.33 % Zn, and an upper zinc-rich zone that has 12.0 Mt averaging 2.33 % Zn and 0.34 % Cu; the gossan contains 1.1 Mt of precious-metal-enriched iron oxides having an average grade of 4.5 g/t Au and 103 g/t Ag (Scully, 1993). During the past two decades over 400 diamond drill cores have been obtained from the deposit and surrounding area, which form the sample basis for the present study. This report is a preliminary account of our study, which has included relogging of drill cores, X-ray

diffractometry of rocks and mineral separates, detailed petrography of doubly polished thin sections, and scanning electron microscope and electron microprobe analyses of ore and gangue minerals.

## REGIONAL SETTING

Country rocks surrounding the Bald Mountain deposit are weakly metamorphosed submarine volcanic and lesser sedimentary rocks that make up the Ordovician Winterville Formation (Scully, 1993). This formation consists of amygdaloidal and massive basalt, with minor interbedded sedimentary rocks (including volcaniclastic facies), rhyolitic tuffs, and agglomerates (Horodyski, 1968). The presence of graptolites within nearby shale units provides a minimum age range for the Winterville from Middle to Late Ordovician (graptolite zones 11-15: Roy and Mencher, 1976, Fig. 12); conodonts in a calcareous siltstone bed from a shale unit 6 km southeast of the deposit are late Llandeilian to early Caradocian (A.G. Harris, person. commun., 1997). Volcanic rocks possibly correlative with those of the Winterville Formation occur in the Bluffer Pond and Munsungan Lake formations in the southern part of the Munsungan inlier approximately 50 km to the southwest of Bald Mountain (cf. Hall, 1970; Berry and Osberg, 1989), and in upper stratigraphic units of the Tetagouche Group ~200 km to the northeast in northern New Brunswick (cf. van Staal et al., 1992; McCutcheon et al., 1997). Geochemical studies of basalts of the Winterville Formation by Winchester and van Staal (1994) suggest deposition within an ensialic back-arc basin, in a setting broadly similar to that of the probably coeval Tetagouche Group.

The Winterville Formation is overlain unconformably by Upper Silurian formations made up of shale, sandstone, conglomerate, fossiliferous limestone, and minor volcanic rock (Horodyski, 1968; Roy and Mencher, 1976). Siliciclastic turbidite deposits of the Seboomook Formation (Lower Devonian) comprise gray to black shale, minor graywacke, and sparse siltstone that lie stratigraphically above the Silurian units, and in map view surround the Winterville Formation (Osberg et al., 1985). The base of the Winterville is not exposed; siliciclastic mélange like that of the Lower Ordovician Chase Brook Formation to the south (Hall, 1970; Berry and Osberg, 1989) could underlie the Winterville Formation, but direct evidence for this is lacking. Intrusive rocks in the region

include a variety of subvolcanic bodies (mainly gabbro and lesser rhyolite) of Ordovician age, and several younger granites of Acadian (Early Devonian) age.

Structural relationships are poorly known. The regional distribution of Paleozoic stratigraphic units shows the Bald Mountain area to lie near the core of the Munsungun-Winterville anticlinorium, a broad Acadian structure that strikes northeast with a gentle northeast plunge (Osberg et al., 1985; Berry and Osberg, 1989). Taconic (Late Ordovician) structures have not been described in central Aroostook County, but could be important locally. Steeply dipping faults of Acadian age are present in places, where they cut strata within the Munsungun-Winterville anticlinorium including various Silurian units and the Lower Devonian Seboomook Formation (Horodyski, 1968; Osberg et al., 1985). The volcanic and intrusive rocks generally lack a cleavage or schistosity except near faults and shear zones; shales of Ordovician through Devonian age uniformly display a well-developed cleavage.

Regional metamorphism of the Bald Mountain area has only reached prehnite-pumpellyite grade (Richter and Roy, 1976; Osberg et al., 1985; Walker and Murphy, 1995). Mafic rocks at and near Bald Mountain are characterized by assemblages of albite + chlorite ± calcite ± prehnite ± pumpellyite ± epidote ± actinolite ± titanite ± pyrite, which to the north show a progressive decrease in metamorphic grade where assemblages contain prehnite and/or pumpellyite, or prehnite and/or analcime, but no actinolite or epidote (Richter and Roy, 1976; Walker and Murphy, 1995). Regional metamorphic temperatures in the deposit area were 300-325°C, based on a conodont alteration index (CAI) of 5 determined by A.G. Harris (person. commun., 1997) on specimens collected from a hangingwall shale sequence 6 km southeast of Bald Mountain.

## DEPOSIT GEOLOGY

### Local setting

The Bald Mountain deposit is within a sequence of variably altered volcanic and minor sedimentary strata of the Winterville Formation (Fig. 2)[1]. Using the nomenclature of Horodyski (1968), the deposit is hosted by the

[1] A revised version of Figure 2, including the area surrounding the Bull Hill prospect to the south, is currently being prepared by M.P. Foose, C.J. Busby, and J.F. Slack.

Greenlaw Mountain member. Rocks in the deep footwall, to the east of the deposit, comprise dark green to greenish-black amygdaloidal pillow basalt and pillow to hyaloclastite breccia, in which vesicles are commonly filled with quartz ± calcite ± pyrite. Small bodies of gabbro occur locally, some of which contain quartz ± epidote veins. Also in the deep footwall is an irregular intrusion of medium-grained, equigranular biotite granite that has an apparent Ordovician age, on the basis of contained epidote-rich quartz veins that are considered deep facies of the Bald Mountain hydrothermal system (Acadian metamorphic epidote is uncommon to rare in the study area). The shallow footwall, within ~100 m of the base of the deposit, comprises pale gray to medium gray rhyolite lapilli tuff. Where unaltered, this tuff is characterized by abundant pumice fragments and few crystals; in places it contains small (<5 cm) to rarely large (1-2 m) angular clasts of aphanitic gray rhyolite. Pale gray spheroidal rhyolite occurs locally near the base of the rhyolite tuff.

The lower part of the hangingwall to the deposit comprises volcanic rocks and a variety of chemical sediments. Overlying the massive sulfides in most places is a distinctive hydrothermal chert up to 28 m thick (Fig. 4) that varies from white to gray to red; lower parts commonly are brecciated and filled with veins composed of pyrite and(or) quartz. Where it contains abundant disseminated hematite, the red chert can be classified a jasper. Locally the chert is separated from the underlying pyrite zone, and from an overlying crystal- and lithic-rich tuff, by an altered lapilli tuff up to several meters thick. In a few places the chert has interlayered dark gray shale units ~10 cm thick that contain multiple laminae of pyrite. Some of the chert, especially the higher stratigraphic parts, appear to be subseafloor replacements of rhyolite tuff, although exhalative portions are believed to predominate. Above the chert is a gray crystal- and lithic-rich tuff commonly 5-20 m thick that contains abundant quartz phenocrysts and sparse feldspar phenocrysts; lithic fragments are small (<5 cm) and comprise aphanitic rhyolite, minor quartz-phyric rhyolite and(or) red chert, and rare basalt that increase in proportion downsection. The tuff is variably altered, and in places contains abundant secondary muscovite. Overlying the tuff is a sequence of mostly massive basalts, with pillow basalts present locally at the base. Very thin layers <10 cm thick of hematite- and magnetite-bearing, reddish-brown shale occur between some basalt flows. The basalts also are variably altered, with plagioclase laths well preserved but pyroxenes completely replaced by chlorite ± pumpellyite (?).

The upper hangingwall to the west of the deposit (Fig. 2) consists of a mixture of sedimentary, volcanic, and intrusive rocks that make up part of the Clayton Lake member of the Winterville Formation of Horodyski (1968). Overlying the immediate hangingwall basalts is a sequence of additional crystal- and lithic-rich rhyolitic tuffs and intercalated basalts, which is succeeded upward (to the west) by dark gray to black carbonaceous shale. Overlying the shale is a unit of fine-grained rhyolitic ash and agglomerate, the latter containing angular to subrounded clasts of rhyolite. Prominent gabbro bodies intrude this rhyolite sequence locally, such as to the west of the deposit. Above the rhyolite sequence, to the immediate west of the area shown in Figure 2, are similar rhyolite agglomerates and tuffaceous graywackes that are intercalated with gray to greenish chert and gray cherty shale, and intruded by (or interlayered with) basalt and diabase.

Geometry

The Bald Mountain deposit comprises several mineralized zones that occur within a local west-dipping sequence along the west end of No Name Ridge[2] (Fig. 2). The deposit is approximately 370 m x 275 m in diameter and up to 215 m thick. A simplified plan map (Fig. 3) shows the massive sulfide body to be bordered by an orthogonal set of steeply-dipping faults that strike northeast and northwest. These faults successively offset the deposit, most prominently at the west end. The northeast-trending faults also offset the smaller CL deposit to the north (Fig. 2), which is believed to be a distal equivalent of the Bald Mountain body. Hypogene sulfide zones of the Bald Mountain deposit are inclined stratabound units that display a broadly conformable geometry with surrounding volcanic rocks, especially in the hangingwall sequence. However, it is noteworthy that these zones are not strictly coplanar with their host strata, as is common in other VMS deposits (e.g., Franklin, 1993, 1995), and at the southwest end (Fig. 4) the zones are enclosed along their projected strike by footwall volcanic rocks.

---

[2] No Name Ridge is informally used here for the east-west ridge to the immediate north of Bald Mountain and to the south of Bishop Mountain. Note that the USGS 7.5-Minute topographic map of the Greenlaw Pond quadrangle (1986) shows Bald Mountain as encompassing both of these ridges, whereas the older (1930) 15-Minute Greenlaw quadrangle restricts Bald Mountain to the area of the southern mountain.

Gossan and supergene zones

A surficial gossan zone underlies an average of 18 m of glacial till. This gossan is nearly horizontal and has a discordant geometry with respect to the inclined hypogene zones below, thus indicating that it formed after tilting of the deposit, probably during the late Tertiary; an Ordovician seafloor weathering origin for the gossan is thus discounted. The gossan consists mainly of porous and friable, red to dark brown aggregates of quartz, goethite, and limonite, with associated gold and silver but little or no base metals (Scully, 1993). Below the gossan is an irregular supergene zone composed mainly of vuggy pyrite and secondary copper minerals, chiefly chalcocite, covellite, and enargite (Lewczuk, 1991). The copper-rich supergene zone lacks zinc concentrations except where supergene processes have overprinted the updip end of the zinc-rich pyrite zone (Scully, 1993).

Hypogene zones and grades

Three major zones of hypogene massive sulfide have been recognized (Scully, 1993). These include a zinc-rich pyrite zone, a copper-rich pyrite zone, and a copper-rich pyrrhotite zone (Figs. 3, 4). The zinc-rich pyrite zone makes up a significant part of the deposit, in the range of ~40-60 volume percent, forming the upper part of the primary sulfide body and in places the lowermost part of the deposit, beneath the copper-rich pyrrhotite zone. Typical grades of the zinc-rich pyrite zone are 1-4 % Zn, <0.5 % Cu, and <0.5 % Pb, with ~10-90 g/tonne Ag and <1 g/tonne Au; rare intervals (5-ft. assay lengths) have up to 8-10 % Zn, whereas others have 1-2 % Pb and(or) 100-200 g/tonne Ag. Gold contents are generally <2 g/tonne, although as much as 3.5 g/tonne Au occurs in a few places, generally near zinc-rich intervals. Whole-rock analyses of five pyritic samples from this zone (Table 1) show 42-160 ppm Ag, 4700 to >10000 ppm As, <10 ppm Bi, 68-240 ppm Cd, <3 ppm Co, 200-690 ppm Cu, 1800-7000 ppm Pb, 440-1900 ppm Sb, and 1.8-3.0 % Zn by semi-quantitative emission spectroscopy; quantitative atomic absorption analyses indicate slightly high Hg (1.5-5.7 ppm) but low Se (<2 ppm), Te (<0.1 ppm), and Au (<0.9 ppm), except for one sample from near the stratigraphic top of the zinc-rich pyrite zone that has 1.8 ppm Au.

The copper-rich pyrite zone is generally found below the zinc-rich pyrite zone and above the pyrrhotite zone; locally the copper-rich pyrite zone occurs below the pyrrhotite zone. The copper-rich pyrite zone comprises

~20-30 volume percent of the primary sulfide body. Grades of this zone are commonly in the range 1-2 % Cu and <0.5 % Zn, with <20 g/tonne Ag and <1 g/tonne Au; rare intervals have 10-15 % Cu. Whole-rock analytical data for three chalcopyrite-rich samples (Table 1) show 54-450 ppm Ag, 310-2900 ppm As, <10 to 87 ppm Bi, <32 ppm Cd, 160-660 ppm Co, 12.0-20.0 % Cu, 120-310 ppm Pb, <220 ppm Sb, 1600-3500 ppm Zn, <0.005 to 3.0 ppm Hg, 350-440 ppm Se, 34-80 ppm Te, and 0.17-0.38 ppm Au.

The copper-rich pyrrhotite zone is distributed along or near the stratigraphically lowest part of the deposit, and makes up ~10-40 volume percent of the primary massive sulfides. Typical grades are 1-2 % Cu and <0.5 % Zn, with <15 g/tonne Ag and <1 g/tonne Au; rare intervals have up to 7-10 % Cu. In most areas, the pyrrhotite content of the copper-rich pyrrhotite zone is less than 30 volume percent, due to extensive overprinting by younger stages of mineralization (see below). One sample of chalcopyrite-rich massive pyrrhotite from this zone (Table 1) contains 18 ppm Ag, 1600 ppm As, <10 ppm Bi, <32 ppm Cd, 510 ppm Co, 8.0 % Cu, 810 ppm Pb, <220 ppm Sb, 1200 ppm Zn, <0.005 ppm Hg, 330 ppm Se, 25 ppm Te, and 0.17 ppm Au.

Footwall feeder zone

The Bald Mountain deposit has a distinctive footwall feeder zone with several types of veins and altered rocks. Most of the feeder zone is developed in rhyolite tuff, although locally the host is amygdaloidal basalt. The feeder zone occurs along the stratigraphic base of the deposit, and varies in thickness from a few meters to nearly 50 m. In detail, there appear to be two separate areas of veins and altered rock, one at a relatively shallow level on the northeast side of the deposit and and the other at a relatively deep level on the southwest side. In both, the texture and mineralogy of the wall rocks commonly is obliterated so that the protolith cannot be easily identified. Characteristic in drill cores are intervals of variably altered (mainly silicified) rhyolite tuff that alternate with pyrite-rich chloritite. The chloritite is composed mainly of dense black chlorite and minor to abundant pyrite, the pyrite forming disseminated euhedral cubes or dodecahedrons up to ~1 cm in diameter, or aggregates of grains in irregular clots 3-10 cm in size. Where the feeder zone is developed within basalt, quartz ± calcite amygdules are partially to completely replaced by pyrite and(or) chalcopyrite. Some intervals contain chloritite that is cut by

chalcopyrite ± pyrite veins; other intervals have abundant muscovite and(or) talc. Less common are white quartz ± chalcopyrite veins, which are younger than the chlorite-rich altered rocks. These quartz-rich feeder veins and associated silicified rocks are believed to be related to Stage III quartz veins and replacements that occur in the overlying massive sulfide body (see below). The feeder zone also locally contains thin (<1 cm) veins composed of magnetite, siderite, or rare hematite within the chloritite and in chlorite-altered footwall rocks; rare 1-3 cm thick veinlets of very fine-grained (aphanitic) quartz, greenalite, and chlorite (± berthierine?) are late hydrothermal products. Sphalerite and galena additionally occur in rare veinlets <1 cm thick, but their paragenesis with respect to other sulfide-bearing veins in the feeder zone is unclear. Veins composed of abundant pyrrhotite and chalcopyrite occur in one area of the footwall, in the northeastern part of the deposit; these may be related to formation of the nearby copper-rich pyrrhotite zone. Grades within the footwall feeder zone are widely variable, but commonly are in the range of 0.5-2.0 % Cu, with local traces of Au; rare intervals have as much as 6.3 % Cu. In general, copper grades increase upward toward the base of the massive sulfide body. Whole-rock analytical data for two chalcopyrite-rich samples from the feeder zone (Table 1) show 6.2 and 9.6 ppm Ag, 270 ppm As, <10 ppm Bi, <32 ppm Cd, 110 ppm Co, 3.0 and 4.0 % Cu, 54 and 120 ppm Pb, <68 ppm Sb, 400 and 500 ppm Zn, <0.005 ppm Hg, 62 and 110 ppm Se, 4.0 and 7.5 ppm Te, and 0.05 and 0.06 ppm Au.

## HYPOGENE MINERAL PARAGENESIS

Exceptional preservation of primary textures in the Bald Mountain deposit has allowed determination of the primary depositional sequence of ore and gangue minerals. This paragenesis, which is unaffected by later deformation and regional metamorphism, is based on several parameters including the distribution of sulfide zones and their relative geometry, on cross-cutting veins and other structures, and on various replacement features that have been documented both megascopically (in drill cores) and microscopically (in polished thin sections). The paragenesis presented here is significantly revised from those reported recently by Slack et al. (1997) and Foley et al. (1997). Seven major stages of hypogene mineralization have been recognized, each of which is described in detail below.

Stage I: exhalative pyrite ± sphalerite ± arsenopyrite ± greenalite deposits

The earliest stage of mineralization (Stage I) is represented by massive pyrite that comprises all of the zinc-rich pyrite zone of the deposit (Figs. 3, 4). This stage is characterized by fine- to medium-grained pyrite with minor amounts of sphalerite, arsenopyrite, and greenalite, plus sparse quartz and other sulfide (and sulfosalt) minerals. The volumetrically dominant pyrite (~70-95 %) typically is massive and structureless, and lacks layering or laminations. Several poorly defined substages have been recognized, which are distinguished chiefly by variations in grain size and color of the pyrite. From oldest to youngest, the substages display the following pyrite types: (Ia) fine-grained brassy pyrite that forms isolated (relict) patches within later Stage Ib pyrite; (Ib) fine-grained to very fine-grained (nearly aphanitic), pale yellowish-brown massive pyrite; (Ic) medium-to coarse-grained yellowish granular pyrite; and (Id) fine-grained yellowish pyrite that occurs as veins within earlier pyrite. Some of the pyrite forms small framboidal grains or displays delicate colloform textures; other pyrite of this stage occurs as very fine-grained aggregates that together display prismatic crystal habits and contain relict cores of pyrrhotite, suggesting pyrite replacement of earlier-formed euhedral pyrrhotite. Bladed euhedral quartz found locally within pyrite aggregates may reflect the sites of former anhydrite crystals that were leached and then replaced by silica. Electron microprobe analyses commonly show ~0.1 wt % Co in the pyrite of this stage.

Sphalerite commonly is interstitial to pyrite and rarely forms thin (to 1 cm) discontinuous layers or laminae; the latter are interpreted as primary textures that formed on the Ordovician seafloor. A minor proportion of the sphalerite occurs as veins <5 mm thick, with or without associated galena, that cut massive pyrite. Preliminary work suggests that much of the sphalerite belongs to the earliest substage(s), especially Ia and Ib, and that it was partially to in places completely removed during subsequent stages of mineralization (Ic and Id). In hand specimen the sphalerite ranges from pale brown to reddish orange to reddish brown; under the microscope, in transmitted light, doubly polished thin sections commonly show delicate growth zoning and open-space filling textures within the sphalerite. Other sphalerite grains are optically homogeneous. Microprobe analyses indicate a

relatively large range of iron contents in the sphalerite, typically from 9.0-14.0 mole % FeS, although as much as 22.0 mole % FeS occurs in some sphalerite of this stage.

Minor constituents of Stage I comprise arsenopyrite, galena, greenalite, minnesotaite, quartz, boulangerite, chalcopyrite, and an unidentified Ag-Sb mineral. Arsenopyrite typically forms white euhedral crystals that are intergrown with or interstitial to pyrite and(or) sphalerite; microprobe analyses show 31.4-34.5 atomic % As. Occurrences of galena are largely restricted to the stratigraphically upper part of the zinc-rich pyrite zone, where it forms small grains intergrown with other sulfides or thin (<1 cm) veins; locally galena occurs in veins <1 cm thick and rarely in 1-3 cm lenses with minor associated sphalerite. Greenalite, a hydrous iron silicate mineral, forms fine-grained, dark greenish black aggregates up to 3 cm in size that typically are interstitial to coarse euhedral pyrite. Another hydrous iron silicate, minnesotaite, occurs as aggregates of tiny needles within greenalite, and in sulfide minerals. Some specimens from this stage also contain trace to minor (up to ~10%) clear or white quartz that forms euhedral to anhedral grains or aggregates; chalcopyrite occurs as sparse disseminated grains and locally contains fine-scale intergrowths of isocubanite (?). Boulangerite, a lead sulfosalt mineral, is closely associated with galena-rich intervals. The Ag-Sb sulfosalt, probably dyscrasite on the basis of optical properties and microprobe data, may be a major carrier for silver in hypogene parts of the deposit. Other mineralogical hosts for silver such as tetrahedrite have not been found, but may exist; some silver could be in solid solution within galena. Gold also is as yet unidentified, but is likely present in this stage owing to preferential stratigraphic dstribution of the Au-bearing gossan zone within the upper part of the zinc-rich pyrite zone (Scully, 1993). The systematically low contents of tellurium in gold-bearing pyritic samples from this zone (Table 1) suggest that gold tellurides are unimportant at Bald Mountain.

Sulfide deposits of Stage I display structures that clearly indicate formation on the Ordovician paleo-seafloor. These structures include distinctive subrounded to rounded clasts of fine-grained pyrite and sparse chalcopyrite, approximately 1-3 cm in diameter, that occur within a matrix of medium- to coarse-grained pyrite. The clasts appear to be restricted to the stratigraphic middle of the zinc-rich pyrite zone, and are interpreted as detritial fragments that became partially to completely rounded by mechanical abrasion during transport on a slope.

Elsewhere in the same stratigraphic interval, fine-grained detrital pyritic material fills former vertical cracks in massive pyrite, suggesting clastic sedimentation of detrital pyrite within fractured parts of a sulfide mound. One partial chimney fragment (cf. Hamon, 1983; Oudin and Constantinou, 1984; Vearncombe et al., 1995) has also been found at the base of the western part of the zinc-rich pyrite zone, enclosed in fine-grained chloritized rhyolite (?). This chimney fragment consists mostly of fine-grained pyrite and shows a concentric structure marked by ~0.5-1.0 cm cores of sphalerite intergrown with thin (<1 mm) laminae and disseminations of chalcopyrite; the original chimney had a diameter of about 5-7 cm. Occurrence of the chimney fragment at the base of the pyrite zone, in contact with altered footwall rocks, is strong evidence for exhalative formation of the stratigraphically lowest (and oldest) part of the deposit.

Evidence also exists for local subseafloor replacement during Stage I mineralization. This replacement is volumetrically minor, however, being restricted to the stratigraphic upper part of the zinc-rich pyrite zone at the southwestern end of the deposit, and locally to the base of the deposit. In the former area, pyrite and local sphalerite (rarely chalcopyrite) display distinctive wispy textures that strongly resemble those of the unaltered lapilli tuff unit, implying replacement of the tuff by sulfides. Similar features are seen in some cores from near the stratigraphic base of the deposit, where textures also suggest sulfide replacement of tuff. However, it is important to note that such replacement textures have not been observed in the many other cores examined (~30) that penetrate the zinc-rich pyrite zone, thus precluding a major role for replacement in forming this portion of the deposit.

Stage II: massive pyrrhotite ± chalcopyrite replacements

Massive pyrrhotite and local massive chalcopyrite are characteristic of Stage II mineralization. This stage occurs only in the copper-rich pyrrhotite zone, which is preferentially found in the stratigraphically lower parts of the deposit (Fig. 4). Most of the pyrrhotite is overprinted by quartz- and pyrite-rich veins of Stages III and IV (see below), so that overall the proportion of pyrrhotite within the copper-rich pyrrhotite zone is only about 20-30 volume percent. In many drill cores, however, short intevals of <1 m consist almost wholly of massive pyrrhotite,

without components of younger Stage III or IV mineralization. The pyrrhotite, which formed during the earlier part of this stage (IIa), is fine-grained as aggregates of anhedral grains that generally make up >95 % of Stage II deposits, except in areas that contain substantial chalcopyrite (IIb). Microprobe analyses show the pyrrhotite to have 47-48 atomic % Fe. In addition to the minor to abundant chalcopyrite, associated minerals (IIb) include minor pyrite and sphalerite, and traces of isocubanite (?) within chalcopyrite. Traces of quartz and greenalite that occur as tiny (<0.1 mm) isolated anhedral grains disseminated within the pyrrhotite are interpreted as unreplaced relicts of Stage I mineralization. Although no direct evidence exists for a replacement origin for the pyrrhotite (or chalcopyrite) of Stage II, several factors argue against its (their) being exhalative. First, the copper-rich massive pyrrhotite zone is restricted to areas near the footwall of the deposit, and is generally close to feeder veins where replacement would have been favored. Second, the anhedral nature of the pyrrhotite differs from the habits of Stage I sulfide minerals that mainly are euhedral to subhedral; pyrrhotite recovered from modern VMS deposits on the seafloor typically forms distinctive euhedral prismatic crystals (e.g., Koski et al., 1984, 1988) that have not been found at Bald Mountain (except as relicts within Stage I mineralization). Third, the formation of pyrrhotite requires reducing conditions in terms of sulfur and oxygen activities, which are unlikely for this stage given the probable oxidizing nature of the water column at that time (see below). The fine-grained and anhedral character of Stage II pyrrhotite is most consistent with a replacement origin, in which the pyrrhotite acquired the preexisting fine-grained texture of Stage Ia and Ib pyrite. Trace amounts of quartz and greenalite that occur within Stage II pyrrhotite may be relicts from Stage I mineralization, and not true components of Stage II. However, the minor to abundant chalcopyrite locally associated with the pyrrhotite is considered an integral part of this stage, although most probably was precipitated slightly after the pyrrhotite. This interpretation provides a basis for subdividing Stage II into the earlier substage containing chiefly massive pyrrhotite (IIa) and the younger substage mainly comprising massive chalcopyrite (IIb). A critical distinguishing feature for identifying Stage II chalcopyrite is the general absence of closely associated (or intergrown) medium- to coarse-grained pyrite, which is characteristic of Stage IV mineralization (see below).

Stage III: irregular quartz veins and replacements

Quartz veins and replacements characterize Stage III mineralization. The veins are irregular and commonly wavy (i.e., lacking a planar structure), suggesting host structures that developed within unlithified sulfide. Typical vein widths are 1-3 cm. Quartz generally makes up >99 % of the veins, although minor (1-5 %) chalcopyrite is present locally. The veins are most abundant in massive pyrrhotite of Stage II, but they also occur locally in medium-grained pyrite of Stage Ic. Within the massive pyrrhotite zone, Stage III quartz veins tend to increase in abundance stratigraphically downward, where they form partial to nearly complete replacements of pyrrhotite; some intervals in drill core in the pyrrhotite zone contain only small remnants of pyrrhotite that make up less than 10 percent of the rock, the remainder consisting of myriad interpenetrating and crosscutting quartz veins and replacements. Within both veins and replacements, the quartz forms distinctive euhedral crystals, in many places showing well-developed pyramidal terminations and trails of fluid inclusions that parallel growth faces of crystals.

Stage IV: pyrite ± chalcopyrite ± magnetite ± quartz ± siderite veins and replacements

Pyrite and chalcopyrite are the major constitutents of Stage IV mineralization. This stage probably formed all of the Cu-rich pyrite zone within the deposit (Fig. 4). The pyrite is uniformly coarse to very coarse in yellowish grains or grain aggregates that occur in distinctive veins and replacements. The veins, about 1-3 cm wide, cut massive pyrrhotite of the pyrrhotite zone (Stage II) and medium-grained pyrite in the lower part of the zinc-rich pyrite zone (Stage I). In most drill core intervals the pyrite is predominant, and has only minor (<10 %) associated chalcopyrite. Elsewhere, however, the proportion of chalcopyrite is substantial (to ~70 %), forming fine-grained, massive concentrations. Locally, the coarse pyrite and chalcopyrite replace Stage I pyrite and Stage II pyrrhotite. The paragenesis of all of the massive chalcopyrite in the deposit is uncertain, though, and it is conceivable that some formed during a separate stage that postdates Stage IV and predates Stage V.

Fine-grained magnetite is a locally abundant constituent of Stage IV. The magnetite forms disseminations, irregular aggregates, and veins <3 cm thick. In short (<10 cm) intervals in drill core the magnetite may be very

abundant, comprising >50 percent of the rock. Commonly the magnetite is intergrown with quartz in paragenetically late domains within or among coarse pyrite aggregates. Texturally similar interstitial fillings in other parts of the deposit contain quartz and siderite. Magnetite does not appear to be associated with the chalcopyrite of this stage, and may be paragenetically younger. The veins of magnetite that occur in the copper-rich pyrite zone are tentatively assigned to Stage IV, but it is possible that these represent later, unrelated veins. The paragenesis of rare veins that contain subequal amounts of magnetite and coarse gray calcite is uncertain; these veins may or may not belong to Stage IV mineralization. Minor sphalerite and arsenopyrite are also tentatively assigned to this stage, although their paragenesis is uncertain.

Stage V: siderite ± quartz ± magnetite ± hematite ± sulfide veins

Distinctive siderite-rich veins make up Stage V mineralization. Veins of this stage occur throughout most of the deposit, including the footwall feeder zone, but are most common in the lower part of the zinc-rich pyrite zone, in the copper-rich pyrite zone, and in the pyrrhotite zone. Morphology of the veins is shown by a wavy to irregular geometry; formation within an unlithified to partially lithified sulfide matrix is implied. The paragenesis of the veins is well established, as they clearly cut veins and replacements of Stages I-IV. Thicknesses range from <1 mm in hairline fracture fillings to ~10 cm in large veins; most are <3 cm wide. The dominant siderite (50-90 vol %) is orange to reddish orange, and makes the veins prominent in hand specimen. Many of the veins are mineralogically zoned, showing a progression from quartz ± sulfide borders to siderite ± magnetite intermediate zones to siderite ± hematite cores. Sulfide minerals are volumetrically very minor (<10 vol %), mainly comprising pyrite and chalcopyrite, but some Stage V veins also contain sparse sphalerite and arsenopyrite; disseminated pyrrhotite, zoned colloform greenalite, and tiny (<0.1 mm) needles of minnesotaite locally occur along borders of the veins. Microprobe analyses show 2.9-11.0 mole % FeS in the sphalerite, 29.8 atomic % As in the arsenopyrite, and 0.1 wt % Co in the pyrite of this stage.

Stage VI: quartz ± chalcopyrite ± pyrite veins

Sparse veins of quartz and sulfide minerals comprise Stage VI. These veins occur from near the top of the zinc-rich pyrite zone to the base of the deposit (lower pyrrhotite zone), but are volumetrically insignificant. Vein widths typically are less than one centimeter. Most of the veins contain quartz together with sparse chalcopyrite and(or) pyrite; some consist wholly of quartz. The veins are irregular and are generally not planar, suggesting that they fill fractures which developed in a matrix (massive sulfide) that was only partially lithified.

Stage VII: barren quartz and calcite veins

Barren quartz and calcite veins comprise Stage VII mineralization. These veins typically are 1-3 cm wide, occur throughout the deposit, and are uncommon to rare. They display a strong planar structure, which implies filling of fractures that cut lithified rock. Stage VII veins clearly are paragenetically very late, and possibly are Acadian in age, although a hydrothermal origin related to Ordovician formation of the Bald Mountain deposit cannot be excluded.

## PRELIMINARY GENETIC MODEL

Field and laboratory work completed to date provide the foundation for a preliminary genetic model of the Bald Mountain deposit. The setting of the deposit within submarine volcanic rocks, its broadly stratabound nature, and the occurrence of massive sulfide material with an overlying hematitic chert unit indicate a volcanogenic origin on or near the Ordovician seafloor (e.g., Lydon, 1988; Franklin, 1993). Unusual geometric relations within the deposit and its inferred faulted margins suggest formation within a seafoor graben or other collapse feature, in which faults that presently border and locally offset the deposit are reactivated synvolcanic faults; some of these faults probably served as major channelways for hydrothermal fluid flow and localized specific types of mineralization and alteration. Our proposed evolution for the deposit involves an episode of major basaltic volcanism followed by the formation of local rhyolite domes that erupted lapilli and other felsic tuffs. Concurrent with or after deposition of the footwall lapilli tuff, steeply-dipping faults developed a graben-type or other collapse

structure. Metalliferous hydrothermal fluids were focused along these faults, depositing massive pyrite and minor sphalerite of Stage I that filled the graben to the level of the seafloor above; time-correlative alteration in the footwall produced chlorite, pyrite, and minor sericite, talc, and chalcopyrite. The general lack of layering or laminations in the Stage I deposits, together with the local presence of abundant sulfide clasts and one chimney fragment, suggest its formation by coelescence of sulfide chimneys and mounds (i.e., proximal mineralization), without deposition from a hydrothermal plume or brine pool (see Hannington et al., 1995). During or soon after deposition of the massive zinc-rich pyrite body (i.e., Stage I deposits), low-temperature fluids precipitated ferruginous siliceous sediments (probably gels) that later were lithified to form the hangingwall hematitic chert unit. This siliceous sediment may have acted as a chemical and thermal seal (Barriga and Fyfe, 1988) above the exhalative pyrite ± sphalerite deposit, promoting subseafloor "zone refining" (e.g., Eldridge et al., 1983; Hannington et al., 1995) that altered mineral assemblages and textures within the zinc-rich pyrite zone. Such zone refining is believed to be responsible for a variety of textures and mineral assemblages observed within Stage I deposits, including the coarse pyrite and interstitial greenalite ± minnesotaite that are interpreted to have formed from reduced Fe- and Si-bearing fluids introduced into the lower portion of the massive pyrite body, after deposition of the hangingwall ferruginous siliceous sediments.

Mineralization that followed precipitation of the ferruginous siliceous sediments occurred entirely beneath the seafloor. Stage II massive pyrrhotite ± chalcopyrite developed preferentially in the lower parts of the deposit, near footwall feeder zones and related growth faults, by replacement of Stage I pyrite. Rare pyrrhotite-rich veins in the footwall are correlated with this replacement. Stage III quartz veins and replacements formed in the massive pyrrhotite and massive pyrite zones while the previously deposited sulfides were unlithified; these quartz-rich facies increase downsection and are interpreted as being genetically related to the quartz-rich veins (and silicified rock) that occur locally in the footwall. Subsurface jasper formation (i.e., by replacement) in the hangingwall chert, and in higher stratigraphic units, also may have occurred at this time. Stage IV pyrite ± chalcopyrite ± magnetite veins and replacements formed soon after, developing some copper-rich portions of the deposit within the lower part of the zinc-rich pyrite zone; where this stage overprints the massive pyrrhotite zone, a dominant reaction may have

been the oxidation of pyrrhotite to form pyrite + magnetite (cf. Krasnov et al., 1994). Influx of $CO_2$-rich fluids was instrumental in the formation of Stage V siderite-rich veins, which developed during conditions of highly variable oxygen activity as indicated by their mineralogy of pyrrhotite, pyrite, magnetite, greenalite, minnesotaite, and local hematite, although the hematite does not coexist with the pyrrhotite and may not coexist with the magnetite or pyrite. Additional subsurface jasper formation, including selective replacement of hangingwall volcanic units, could have taken place from these oxidized fluids. Stages VI and VII, which are volumetrically unimportant, formed during the waning stages of the hydrothermal system (VI) and(or) possibly much later during the Acadian orogeny (VII).

## ACKNOWLEDGMENTS

We thank T. Jensen and Black Hawk Mining Inc. (Toronto) for access to surface exposures, drill cores, and exploration reports, as well as permission to carry out this study. The geological framework for our mineralogical and paragenetic investigation has benefitted greatly from the many maps and sections prepared by geologists from J.S. Cummings Inc., Superior Mining Company, and Chevron Resources Company. Appreciation is extended to J.C. Finch and Cominco-American Resources Inc. (Spokane) for supplying reconnaissance outcrop maps of the surrounding region, and to R.L. Parsley (Tulane University) for providing thesis maps and field notes made by the late R.J. Horodyski; J.J. Kowalik and Newmont Exploration Ltd. (Denver), and P.T. LaPierre and the former Superior Mining Company (Bangor), donated drill cores for analysis. We acknowledge many fruitful discussions with other members of the USGS Bald Mountain Study Group: R.A. Ayuso, C.J. Busby, N.K. Foley, M.P. Foose, K.J. Schulz, and R.R. Seal II. Thanks also to R.G. Marvinney and H.N. Berry IV of the Maine Geological Survey for interest and encouragement. H.T. Evans Jr. (USGS) acquired X-ray diffraction data that confirmed identification of the greenalite and minnesotaite; A.G. Harris (USGS) identified conodonts. Assistance in the field and during core logging was provided by J.M. Coder, B.C. Hearn, Jr., J.D. Hersh, E.R. Jones, M.B. Lear, and J.H. McCarthy. The manuscript was improved by the reviews of R.R. Seal II and W.C. Shanks III.

## REFERENCES CITED

Barriga, F.J.A.S., and Fyfe, W.S., 1988, Giant pyritic base-metal deposits: the example of Feitais (Aljustrel, Portugal): Chemical Geology, v. 69, p. 331-343.

Berry, H.N., IV, and Osberg, P.H., 1989, A stratigraphic synthesis of eastern Maine and western New Brunswick, *in* Tucker, R.D., and Marvinney, R.G., eds., Studies in Maine Geology: Augusta, Maine, Maine Geological Survey, v. 2, p. 1-32.

Cummings, J.S., 1988, Geochemical detection of volcanogenic massive sulphides in humid-temperate terrain (using surficial methods): Bangor, Maine, J.S. Cummings, Inc., 298 p.

Eldridge, C.S., Barton, P.B., Jr., and Ohmoto, H., 1983, Mineral textures and their bearing on formation of the Kuroko orebodies, *in* Ohmoto, H., and Skinner, B.J., eds., The Kuroko and related volcanogenic massive sulfide deposits: Economic Geology Monograph 5, p. 241-281.

Feiss, P.G., and Slack, J.F., 1989, Mineral deposits of the U.S. Appalachians, *in* Hatcher, R.D., Jr., Thomas, W.A., and Viele, G.W., eds., The Appalachian-Ouachita orogen: Geological Society of America, Decade of North American Geology, v. F-2, p. 471-494.

Foley, N.K., Slack, J.F., and Flohr, M.J.K., 1997, Fluid evolution and mineral deposition in the Bald Mountain volcanogenic massive sulfide deposit, northern Maine (abs.): Geological Society of America, Abstracts with Programs, v. 29, no. 6, p. A-59.

Franklin, J.M., 1993, Volcanic-associated massive sulphide deposits, *in* Kirkham, R.V., Sinclair, W.D., Thorpe, R.I., and Duke, J.M., eds., Mineral deposit modeling: Geological Association of Canada, Special Paper 40, p. 315-334.

Franklin, J.M., 1995, Volcanic-associated massive sulphide base metals, *in* Eckstrand, O.R., Sinclair, W.D., and Thorpe, R.I., eds., Geology of Canadian mineral deposit types: Geological Survey of Canada, Geology of Canada, No. 8, p. 158-183 [also DNAG Volume P-1].

Fyffe, L.R., van Staal, C.R., and Winchester, J.A., 1990, Late Precambrian-early Paleozoic volcanic regimes and associated massive sulphide deposits in the northern mainland Appalachians: Canadian Institute of Mining and Metallurgy Bulletin, v. 83, p. 70-78.

Gair, J.E., and Slack, J.F., 1979, Map showing lithostratigraphic and structural setting of stratabound (massive) sulfide deposits in the U.S. Appalachians: U.S. Geological Survey Open-File Report 79-1517, scale 1:1,000,000 [4 map sheets].

Gair, J.E., and Slack, J.F., 1980, Stratabound massive sulfide deposits of the U.S. Appalachians, *in* Vokes, F.M., and Zachrisson, E., eds., Caledonian-Appalachian stratabound sulphides: Geological Survey of Ireland, Special Paper No. 5, p. 67-81.

Hall, B.A., 1970, Stratigraphy of the southern end of the Munsungun anticlinorium, Maine: Maine Geological Survey Bulletin 22, 63 p.

Hamon, R.M., 1983, Growth history of hydrothermal black smoker chimneys: Nature, v. 301, p. 695-698.

Hannington, M.D., Jonasson, I.R., Herzig, P.M., and Petersen, S., 1995, Physical and chemical processes of seafloor mineralization at mid-ocean ridges, *in* Humphris, S.E., Zierenberg, R.A., Mullineaux, L.S., and Thomson, R.E., eds., Seafloor hydrothermal systems: Physical, chemical, biological, and geological interactions: American Geophysical Union Monogaph 91, p. 115-157.

Horodyski, R.J., 1968, Bedrock geology of portions of Fish River Lake, Winterville, Greenlaw, and Mooseleuk Lake quadrangles, Aroostook County, Maine: Unpublished M.S. thesis, Massachusetts Institute of Technology, Cambridge, Massachusetts, 192 p.

Koski, R.A., Clague, D.A., and Oudin, E., 1984, Mineralogy and chemistry of massive sulfide deposits from the Juan de Fuca Ridge: Geological Society of America Bulletin, v. 95, p. 930-945.

Koski, R.A., Shanks, W.C., III, Bohrson, W.A., and Oscarson, R.L., 1988, The composition of massive sulfide deposits from the sediment-covered floor of Escanaba Trough, Gorda Ridge: Implications for depositional processes: Canadian Mineralogist, v. 26, p. 655-673,

Krasnov, S., Stepanova, T., and Stepanov, M., 1994, Chemical composition and formation of a massive sulfide deposit, Middle Valley, northern Juan de Fuca Ridge (Site 856), *in* Mottl, M.J., Davis, E.E., Fisher, A.T., and Slack, J.F., eds., Proceedings of the Ocean Drilling Program, Scientific Results: College Station, Texas, Ocean Drilling Program, v. 139, p. 353-372.

Lewczuk, L., 1991, Mineralogical investigation of samples from the Bald Mountain deposit: Unpublished report for Boliden Resources Inc., 77 p.

Lydon, J.W., 1988, Volcanogenic massive sulphide deposits. Part 2: Genetic models: Geoscience Canada, v. 15, p. 43-65.

McCutcheon, S.R., ed., 1993, Lower Paleozoic VMS deposits of Maine: Bathurst '93, Third Annual Field Conference, Geological Society of the Canadian Institute of Mining, Metallurgy and Petroleum, 42 p.

McCutcheon, S.R., Gower, S.J., Lentz, D.R., Langton, J.P., Walker, J.A., Wilson, R.A., Fyffe, L.R., Hamilton, A., and Luff, W.M., 1997, Geology and massive sulphides of the Bathurst Camp, New Brunswick: Geological Association of Canada-Mineralogical Association of Canada, Field Trip B7 Guidebook, 85 p.

Osberg, P.H., Hussey, A.M., Jr., and Boone, G.M., eds., 1985, Bedrock geologic map of Maine: Augusta, Maine, Maine Geological Survey, scale 1:500,000.

Oudin, E., and Constantinou, G., 1984, Black smoker chimney fragments in Cyprus sulphide deposits: Nature, v. 308, p. 349-353.

Richter, D.A., and Roy, D.C., 1976, Prehnite-pumpellyite facies metamorphism in central Aroostook County, Maine, *in* Lyons, P.C., and Brownlow, A.H., eds., Studies in New England geology: Geological Society of America Memoir 146, p. 239-261.

Roy, D.C., and Mencher, E., 1976, Ordovician and Silurian stratigraphy of northeastern Aroostook County, Maine, *in* Page, L.R., ed., Contributions to the stratigraphy of New England: Geological Society of America Memoir 148, p. 25-52.

Scully, M.V., 1993, The Bald Mountain massive-sulfide deposit, Aroostook County, Maine, *in* McCutcheon, S.R., ed., Lower Paleozoic VMS deposits of Maine: Bathurst '93, Third Annual Field Conference, Geological Society of the Canadian Institute of Mining, Metallurgy and Petroleum, p. 3-12.

Slack, J.F., Flohr, M.J.K., and Scully, M.V., 1997, Multistage sulphide-silicate-oxide-carbonate mineralization in the Bald Mountain Cu-Zn-Au-Ag deposit, northern Maine, U.S.A. (abs.), *in* Barriga, F.J.A.S., ed., SEG Neves Corvo Field Conference 1997, Lisbon, Portugal: Society of Economic Geologists, Abstracts and Program, p. 58.

Stephens, M.B., Swinden, H.S., and Slack, J.F., 1984, Correlation of massive sulfide deposits in the Appalachian-Caledonian orogen on the basis of paleotectonic setting: Economic Geology, v. 79, p. 1442-1478.

van Staal, C.R., Fyffe, L.R., Langton, J.P. and McCutcheon, S.R., 1992, The Ordovician Tetagouche Group, Bathurst Camp, northern New Brunswick, Canada: History, tectonic setting and distribution of massive-sulphide deposits: Exploration and Mining Geology, v. 1, p. 93-103.

Vearncombe, S., Barley, M.E., Groves, D.I., McNaughton, N.J., Mikucki, E.J., and Vearncombe, J.R., 1995, 3.26 Ga black smoker-type mineralization in the Strelley belt, Pilbara Craton, Western Australia: Journal of the Geological Society, v. 152, p. 587-590.

Walker, J.R., and Murphy, M.P., 1995, Chloritic minerals from prehnite-pumpellyite facies rocks of the Winterville Formation, Aroostook County, Maine, *in* Schiffman, P., and Day, H.W., eds., Low-grade metamorphism of mafic rocks: Geological Society of America Special Paper 296, p. 141-156.

Winchester, J.A., and van Staal, C.R., 1994, The chemistry and tectonic setting of Ordovician volcanic rocks in northern Maine and their relationship to contemporary volcanic rocks in northern New Brunswick: American Journal of Science, v. 294, p. 641-662.

## FIGURE CAPTIONS

Figure 1. Location map of the Bald Mountain deposit in Aroostook County, northern Maine. Modified from Scully (1993).

Figure 2. Geologic map of the area surrounding the Bald Mountain deposit. Modified from Scully (1993).

Figure 3. Simplified geologic plan of the Bald Mountain deposit at 800-ft (244 m) elevation (modified from Scully, 1993), showing the locations of key drill cores used in the paragenetic analysis. Line A-A′ is along section 550 SE shown on Figure 4; note that the gossan is absent at and below this elevation.

Figure 4. Geologic cross section of the Bald Mountain deposit along section 550 SE, showing the locations of key drill cores (see Fig. 3 for line of section). Modified from Scully (1993).

Figure 5. Hypogene mineralogy and paragenesis of the massive sulfide portion of the Bald Mountain deposit.

## TABLE CAPTION

Table 1. Whole-rock analyses (in ppm) of sulfide-rich samples from the Bald Mountain massive sulfide deposit, Aroostook County, Maine.

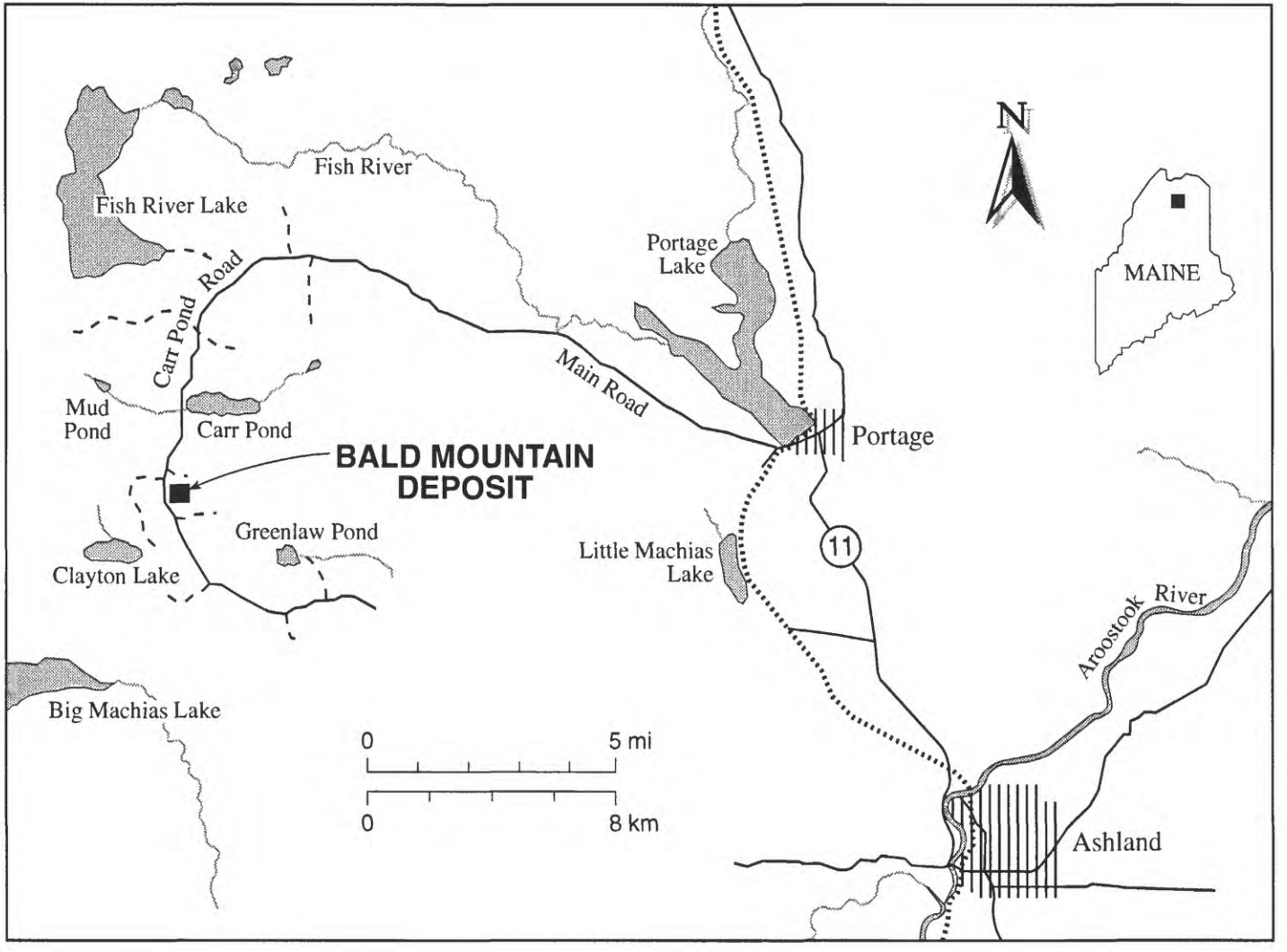


Figure 1. Location map of the Bald Mountain deposit in Aroostook County, northern Maine. Modified from Scully (1993).

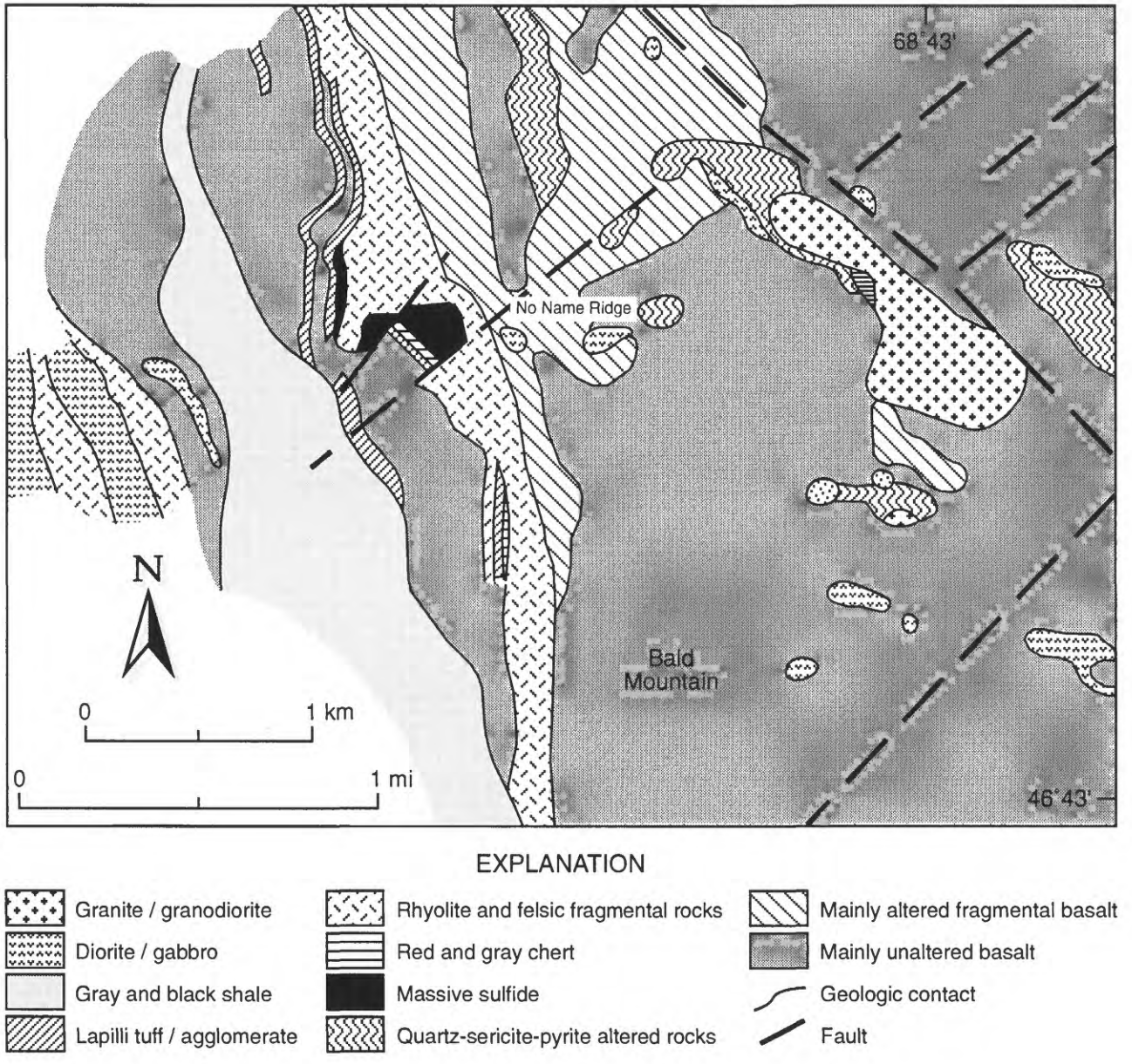


Figure 2. Geologic map of the area surrounding the Bald Mountain deposit. Modified from Scully (1993).

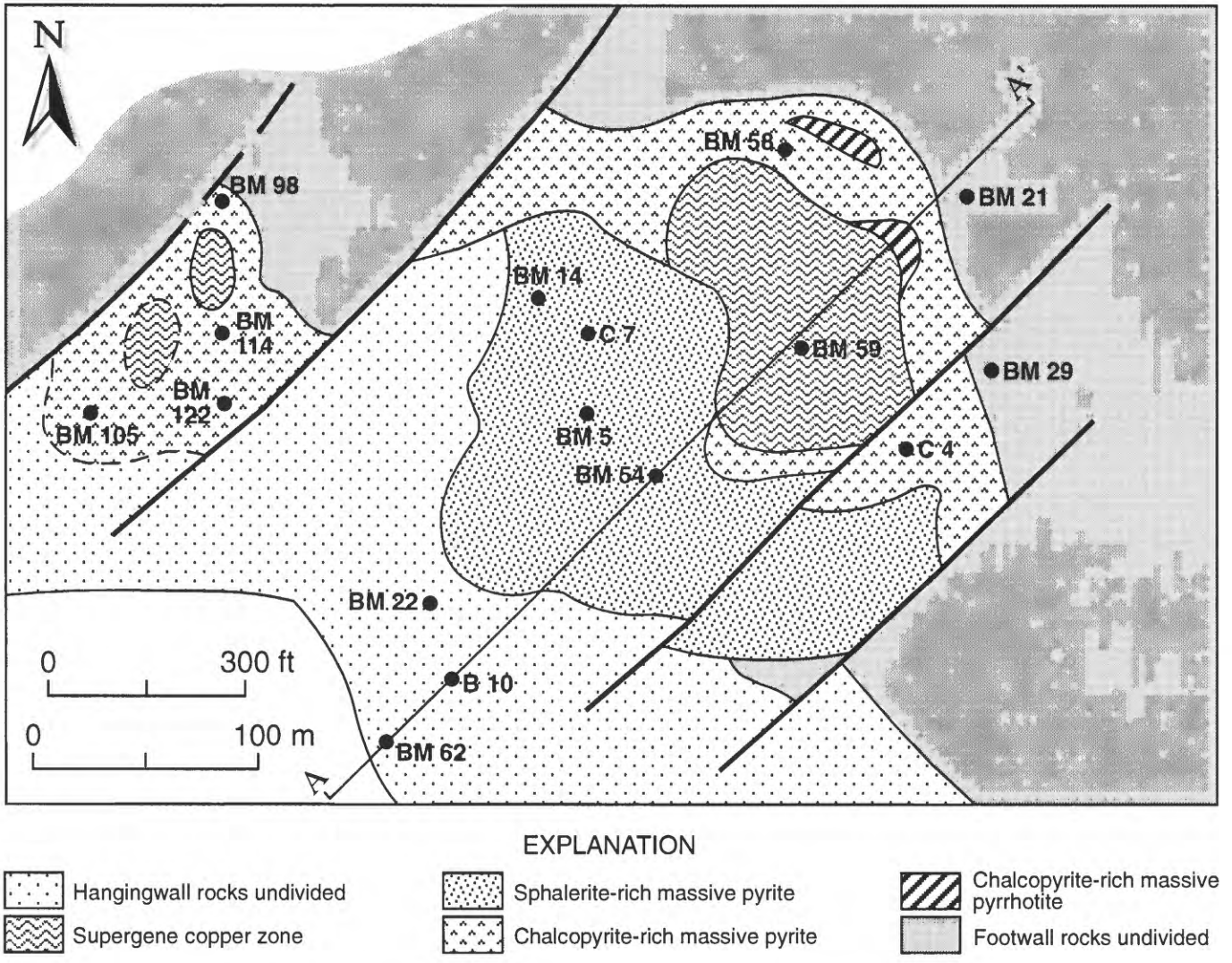


Figure 3. Simplified geologic plan of the Bald Mountain deposit at 800-ft (244 m) elevation (modified from Scully, 1993), showing the locations of key drill cores used in the paragenetic analysis. Line A-A' is section 550 SE shown on Figure 4; note that the gossan is absent at and below this elevation.

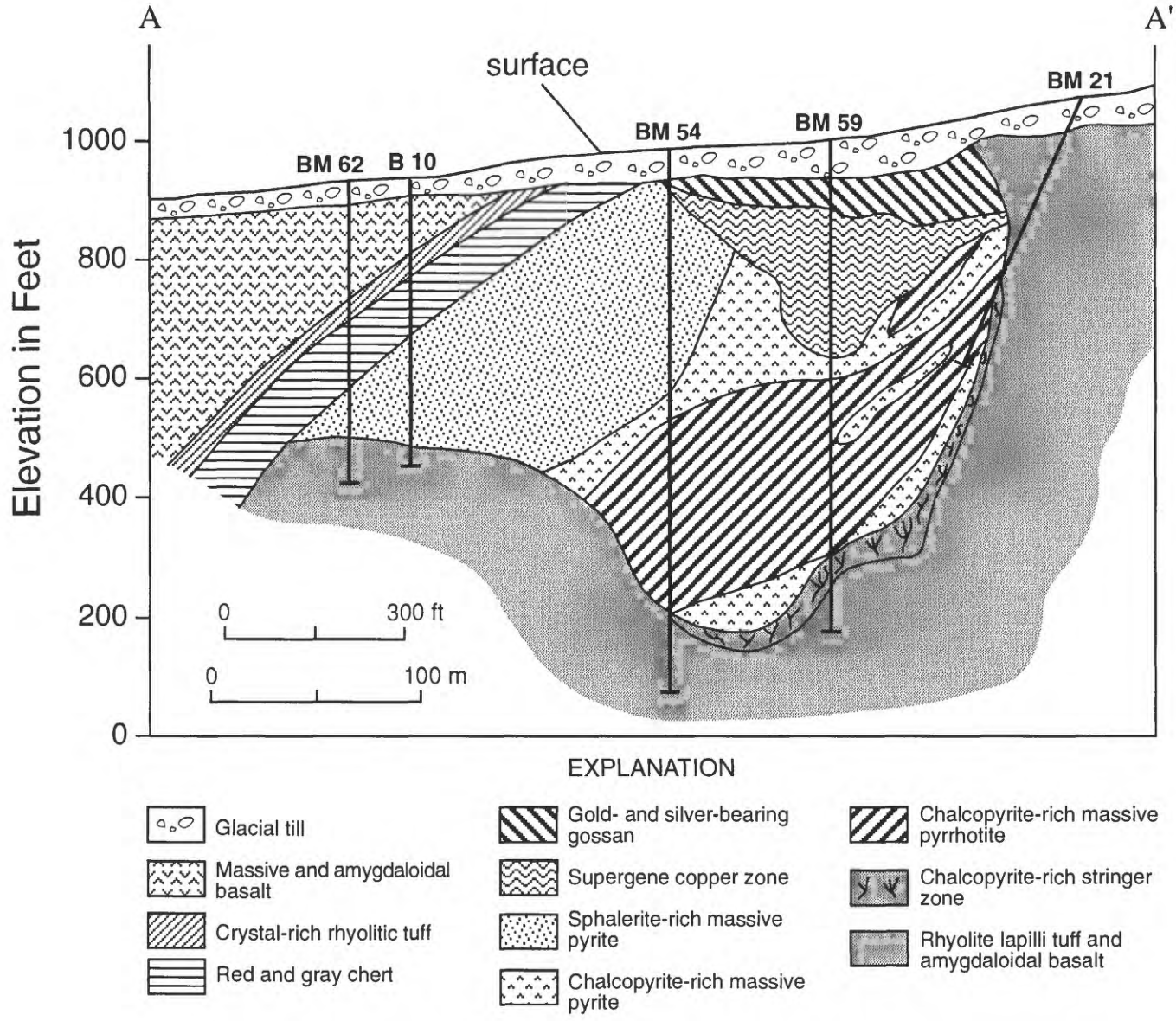


Figure 4. Geologic cross section of the Bald Mountain deposit along section 550 SE, showing the locations of key drill cores (see Fig. 3 for line of section). Modified from Scully (1993).

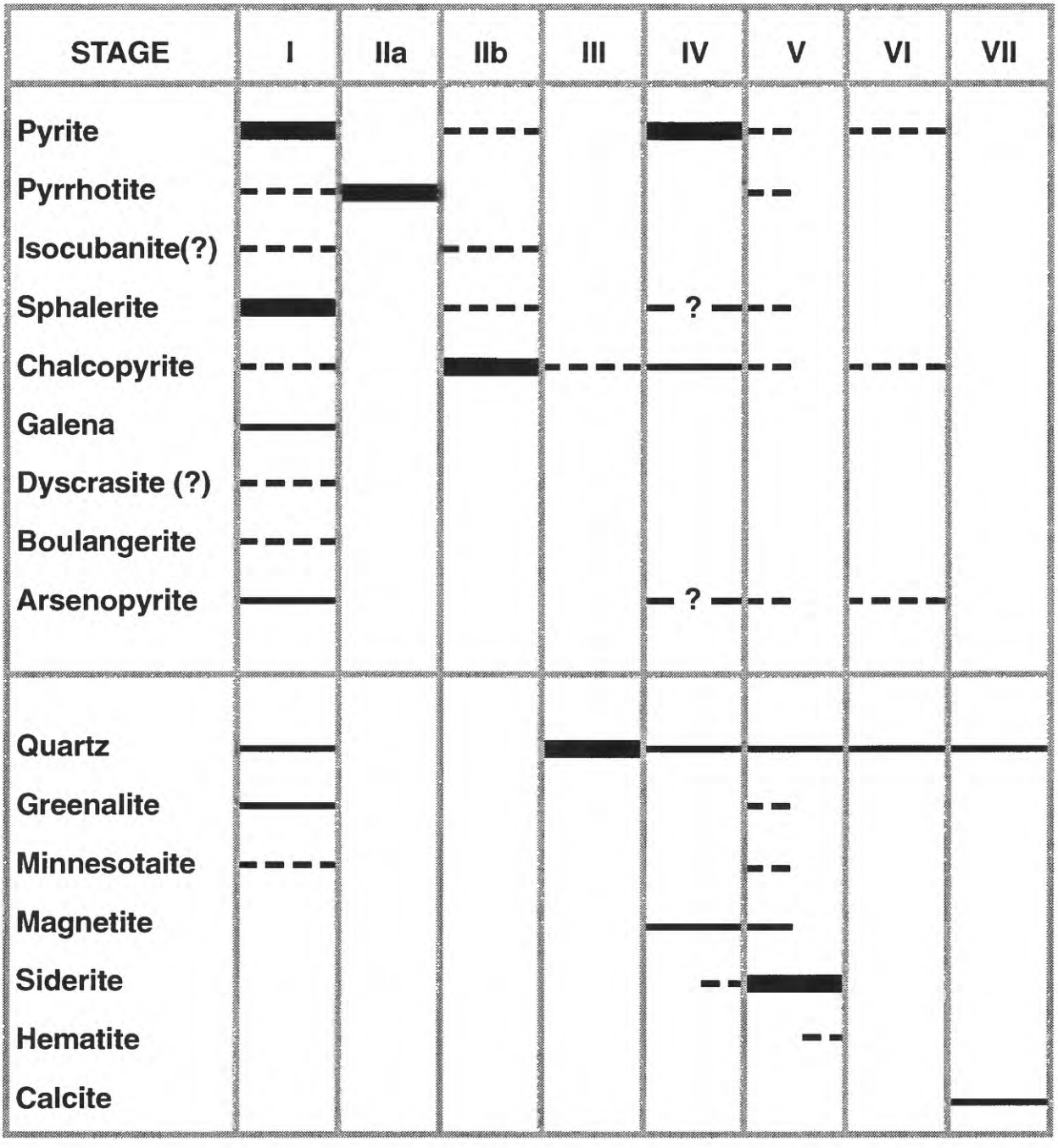


Figure 5. Hypogene mineralogy and paragenesis of the massive sulfide portion of the Bald Mountain deposit.

Table 1. Whole-rock analyses (in ppm) of sulfide-rich samples from the Bald Mountain massive sulfide deposit, Aroostook County, Maine*

| Sample No.# | BM 5/129 | BM 22/220 | BM 22/262 | BM 22/281 | BM 22/299 | BM 21/367 | BM 21/405 | BM 21/454 | BM 21/391 | BM 21/465 | BM 21/497 |
|---|---|---|---|---|---|---|---|---|---|---|---|
| Zone | Zn-pyrite | Zn-pyrite | Zn-pyrite | Zn-pyrite | Zn-pyrite | Cu-pyrite | Cu-pyrite | Cu-pyrite | Cu-pyrrhotite | Footwall | Footwall |
| Ag | 42 | 160 | 90 | 160 | 160 | 73 | 54 | 450 | 18 | 10 | 6 |
| As | 4700 | >10000 | 1600 | 6100 | 7400 | 1200 | 2900 | 310 | 1600 | 270 | 270 |
| Au | 0.08 | 1.8 | 0.06 | 0.43 | 0.82 | 0.38 | 0.17 | 0.17 | 0.17 | 0.05 | 0.06 |
| Ba | 5 | 5 | 2 | 3 | 3 | 21 | 3 | <1.5 | 2 | 10 | 8 |
| Bi | <10 | <10 | <10 | <10 | <10 | 44 | 87 | <10 | <10 | <10 | <10 |
| Cd | 81 | 140 | 260 | 68 | 240 | <32 | <32 | <32 | <32 | <32 | <32 |
| Ce | 140 | <200 | 130 | <200 | <200 | <200 | <200 | <200 | <200 | 85 | 100 |
| Co | 2 | <1 | <1 | 2 | 2 | 660 | 650 | 160 | 510 | 110 | 110 |
| Cr | 2 | <10 | <1 | <10 | <10 | <10 | <10 | <10 | <10 | <1 | 3 |
| Cu | 200 | 690 | 240 | 320 | 370 | 120000 | 180000 | 200000 | 80000 | 40000 | 30000 |
| Ga | <1.5 | H | 3 | H | H | H | H | H | H | 2 | 5 |
| Ge | <4.6 | <4.6 | <4.6 | <4.6 | <4.6 | <4.6 | <4.6 | <4.6 | <4.6 | <4.6 | 5.4 |
| Hg | 1.5 | 4.6 | 5.7 | 2.6 | 4.0 | 3.0 | <0.005 | <0.005 | <0.005 | <0.005 | <0.005 |
| La | <10 | <10 | <10 | <10 | <10 | <22 | 19 | <22 | 26 | <22 | 35 |
| Mn | 130 | 450 | 720 | 660 | 140 | 580 | 390 | 73 | 210 | 140 | 400 |
| Mo | 8 | H | 4 | H | H | H | H | H | H | 2 | 2 |
| Nb | 7 | <6.8 | <6.8 | <6.8 | <6.8 | 11 | <6.8 | 8 | 9 | 7 | 9 |
| Nd | 50 | <32 | <32 | <32 | <32 | <32 | <32 | <32 | <32 | 40 | 34 |
| Ni | 27 | 17 | <1.5 | 3 | <1.5 | <1.5 | 22 | <1.5 | <1.5 | 3 | 4 |
| Pb | 1800 | 5000 | 7000 | 2000 | 2500 | 280 | 310 | 120 | 810 | 120 | 54 |
| Sb | 440 | 780 | 600 | 1900 | 1100 | <220 | <220 | <220 | <220 | <68 | <68 |
| Sc | 1 | <1 | 1 | <1 | 2 | <1 | 2 | <1 | 3 | 4 | 6 |
| Se | 0.7 | 1.3 | <0.1 | 1.5 | 0.5 | 350 | 440 | 440 | 330 | 110 | 62 |
| Sn | 12 | H | 22 | H | H | H | H | H | H | 8 | 6 |
| Sr | <1 | <1 | <1 | <1 | <1 | 2 | <1 | <1 | <1 | 2 | <1 |
| Te | <0.1 | <0.1 | <0.1 | <0.1 | <0.1 | 34 | 80 | 68 | 25 | 7.5 | 4.0 |
| V | 3 | 21 | 3 | 10 | 4 | 4 | <1 | 5 | 3 | 5 | 9 |
| Y | 4 | 6 | 2 | 5 | 4 | 6 | 9 | 6 | 6 | 8 | 8 |
| Yb | 1.4 | 1.7 | 0.34 | 1.8 | <1.0 | 2.0 | 1.9 | 2.0 | 2.7 | 0.44 | 0.42 |
| Zn | 18000 | 20000 | 26000 | 18000 | 30000 | 1600 | 1800 | 3500 | 1200 | 400 | 500 |
| Zr | <3.2 | 13 | 4 | <3.2 | 5 | <3.2 | <4.6 | <4.6 | <3.2 | <3.2 | <3.2 |

*All analyses by semi-quantitative emission spectroscopy except Au, Hg, Se, and Te that are by quantitative atomic absorption; C.J. Skeen, B.S. Spillare, J. Gillison, R. Moore, and P. Aruscavage, USGS analysts. Elements sought but not found, and their lower limits of detection (in parentheses): B (6.8 ppm), Be (1.0 ppm), Dy (22 ppm), Er (4.6 ppm), Eu (2.2 ppm), Gd (32 ppm), Hf (15 ppm), Ho (6.8 ppm), In (10 ppm), Ir (15 ppm), Lu (15 ppm), Os (15 ppm), Pd (1.0 ppm), Pr (100 ppm), Pt (2.2 ppm), Re (10 ppm), Rh (2.2 ppm), Ru (2.2 ppm), Sm (10 ppm), Ta (320 ppm), Tb (32 ppm), Th (46 ppm), Tl (10 ppm), Tm (4.6 ppm), U (220 ppm), W (15 ppm). H = analytical interference (no data).

#Sample numbers are abbreviations for drill cores (BM series) followed by depths, rounded to the nearest foot.